Modelling the Geothermal Energy Potential of Rafin Rewa Warm Spring Region, Precambrian Basement Complex, Nigeria, Using Integrated Aeromagnetic Geophysical Techniques

Ayatu Ojonugwa Usman*[1], Ema Michael Abraham[1], Churchill Chukwunonso Okonkwo[2], Augustine Ifeanyi Chinwuko[3] and George-Best Azuoko[1]

[1]Applied Geophysics Program, Alex Ekwueme Federal University, Ikwo, Ebonyi, Nigeria
[2]Department of Physics, Federal College of Technology, Umunze, Nigeria
[3]Department of Applied Geophysics, Nnamdi Azikiwe University, Awka, Nigeria

ABSTRACT

The geothermal energy potentials of the Rafin Rewa warm spring (RRWS) region Precambrian Basement Complex, Nigeria has been modelled and evaluated with the view of assessing the thermal potential as an alternative energy source to our country Nigeria. Four high resolution aeromagnetic dataset were acquired, analyzed, and interpreted using integrated aeromagnetic geophysical techniques of spectral analysis and Euler deconvolution. Qualitative interpretation of the residual anomalous map reveals a distribution of positive anomalies (> 53 nT) majorly in the central and southeastern regions, which are traced to the granitic rocks, while the low anomalies (< -1.5 nT) have been traced to the RRWS location emanating from the coastal plain sands of the Pliocene, Pleistocene, Oligocene, and Miocene ages. Quantitatively, the depth to the top (DTT) of the anomalous bodies reveals a depression that is almost intersecting with the Curie point depth (CPD) plot at the RRWS location, which indicates high heat flow in the RRWS region. The Spectral Analysis results reveal that the DTT and CPD in this area ranges from 0.512 to 0.761 km and 6.504 to 10.582 km, respectively while the average CPD is 8.543 ± 0.325 km. It is observed that the DTT and CPD decrease as one move away from the RRWS region. The computed heat flow average was 160.76±19.09 mW/m2 within the RRWS region. Euler deconvolution result reveals the presence of geological structures, which were interpreted as faults and fractures with the major fractures trending east-west (E-W) directions, while the minor fractures trend in the northeast-southwest (NE-SW) directions. Geochemical examinations show iconic compositions impacting convective heat transfer processes of the RRWS system. The geochemical result presented shows that iconic compositions impact the convective heat transfer processes associated with geothermal systems. We recommend the areas with shallow CPD for future geothermal energy exploration and exploitation.

Keynote: Geothermal energy; Rafin Rewa; Spectral Analysis Structural Modelling; Aeromagnetic data

INTRODUCTION

Nigeria is currently facing a severe energy crisis, where electricity demand significantly surpasses the available supply. This growing energy deficit has spurred the urgent need to explore alternative energy sources, particularly renewable options. The country's heavy dependence on electricity as its primary energy source has slowed its economic growth and development. Although the Nigerian Federal Government privatized six electricity generation companies and eleven distribution companies in 2013, power generation remains inadequate. By the end of that year, Nigeria's power output averaged 3,800 MW, rising marginally to 3,900 MW in 2014. However, this is far from sufficient for a population exceeding 170 million people (Abraham & Nkitnam, 2017; Abdelrahman et al., 2023; Eldosouky *et al.,* 2023). The power shortage continues, exacerbated by the country's growing population.

To tackle this challenge, exploring alternative energy solutions is crucial. Energy experts estimate that Nigeria needs an investment of $100 billion over the next 20 years to bridge the power gap (Wikipedia, 2016). Research by Abraham *et al.* (2018, 2015) highlights that although large-scale investments in the power sector are essential to ensure reliable and sustainable electricity, securing such funding is difficult given the country's current economic situation.

This study marks the first comprehensive investigation

The authors wish to thank NNPC Limited, NNPC Upstream Investment Management Services (NUIMS), Applied Geophysics Program, Alex Ekwueme Federal University, Ikwo, Ebonyi, Nigeria, Department of Physics, Federal College of Technology, Umunze, Nigeria, Department of Applied Geophysics, Nnamdi Azikiwe University, Awka, Nigeria and NAPE for providing the platform to present the paper during the Annual Conference.

into the geothermal energy potential of the Rafin Rewa Warm Spring (RRWS) region, which has remained unexplored until now. With an average surface temperature of 42.2 °C, RRWS ranks among Nigeria's hottest springs. Previous studies have focused on other warm springs, with surface temperatures ranging from 30 to 54 °C, in areas like Warri and Akiri (Chukwu *et al.*, 2017; Ekwok *et al.,* 2022) (Fig. 1). The geothermal potential in this region is promising. Our assessment will employ magnetic geophysical techniques such as Euler deconvolution, spectral analysis (SA), and analytical signal (AS) to examine the geothermal characteristics of the RRWS region and better understand the basin geomorphology responsible for thermal activity. Additionally, combining Curie depth point (CDP) and Euler structural models will help pinpoint areas suitable for potential drilling. The outcomes of this study will contribute to Nigeria's efforts in developing geothermal energy as part of the country's Renewable Energy Master Plan, helping to meet long-term renewable energy targets.
Geology of the researched region

The study area is situated in central Nigeria, at the southwestern edge of the Jos Plateau, near the Lisiwa ring complex (Fig. 2). Geologically, this region is characterized by Jurassic-era "Younger Granites," which form prominent ring complexes made up of diverse rock types. These include sodalite, amphibole, biotite, linear granite, syenite, and trachyte, with smaller intrusions of gabbro and dolerite. Less commonly, rhyolite, clast deposits, and ignimbrites are preserved (Fig. 2). The ring complexes often overlap, with most intrusions trending southward. Although the complex exhibits a northeastern alignment, there is no clear surface connection between the research site and major regional crustal structures, though this alignment may reflect weaknesses in the underlying basement rock (Obaje, 2009).

The study area lies within the broader Pan-African orogenic belt, which shaped southern Nigeria during the late Proterozoic to early Paleozoic periods. The dominant rocks in this area are igneous, primarily composed of plagioclase mica, quartz, and feldspar, along with smaller amounts of amphibole, biotite, and hornblende. In its fresh state, the rock is typically gray to pink but weathers to deep red or purple (Nwajide, 2005). The Younger Granites were formed during the Pan-African orogeny, a tectonic event that resulted from the collision of the Congo and West African cratons. This collision subjected the Jos Plateau rocks to intense heat and pressure, causing them to melt and form the Younger Granites. These granites are widespread across the plateau, with notable outcrops in areas like Jos, Bukuru, and Kanam. Due to its strength and resilience, the Younger Granite is widely used as a construction material, contributing to the region's architectural and geological significance. It is used for roads, monuments, and unique rock formations, adding to the Jos Plateau's distinct landscape.

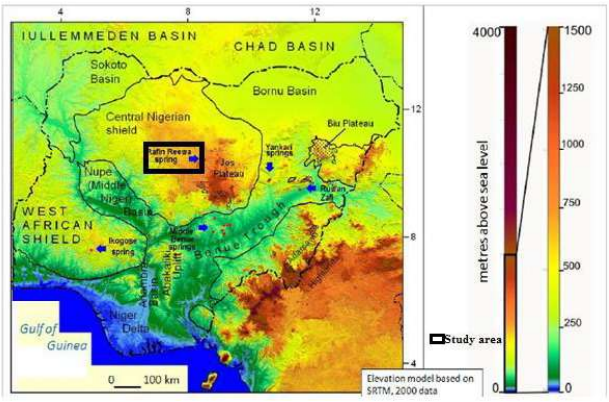

Figure 1: Location map of the study area over Nigeria geothermal Hot Spring. Map

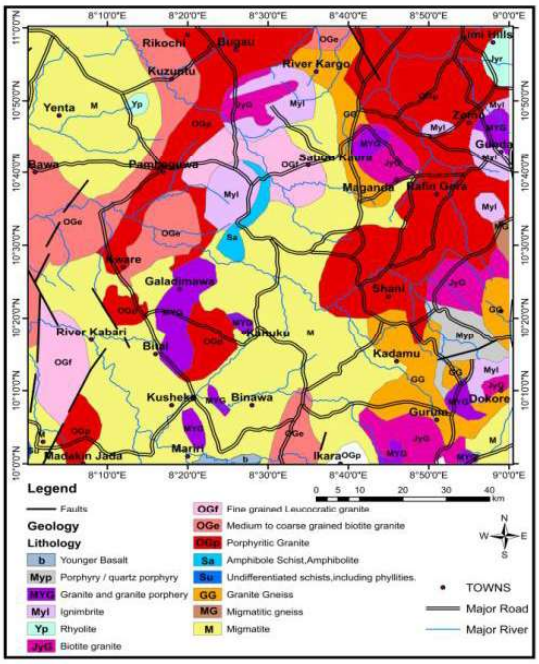

Figure 2: Local Geology map of the research region.

MATERIAL AND METHOD

Aeromagnetic Data (HRAM) sets, specifically sheets 126 Dutsen Wai, 126 Ririwai, 146 Bital, and 147 Rahama, were the input data used in this work. The data was acquired from the Nigerian Geological Survey Agency in Abuja (NGSA) and had already been converted to digital form, with a line spacing of 500 m along a flight line spanning 2 km. Prior to the utilization of the HRAM, the ambient magnetic field and diurnal magnetic effects were removed from the data. The HRAM data sets were integrated and contoured to produce the Total Magnetic Intensity (TMI) anomalous map.

Integrated geophysical techniques were utilized to interpret and model the local anomalies from the data. It is

worthy to note that no single geophysical method can provide conclusive results or recommendations; thus, the combination of different geophysical techniques is essential to increase the confidence level in the interpretation. In this particular study, spectral analysis and Euler deconvolution techniques were integrated into the thermal depth calculations and subsurface structural modeling. The spectral analysis technique involved the use of digitized residual anomalous map (RAM) data, which was then converted into a Fourier domain to compute the energy spectrum.

The mathematical background of the Spectral analysis was summarized by Chinwuko *et al.* (2004) and shown below:

$$Y_{i(x)} = \sum_{n=1}^{N}\left[a_n \cos\left(\frac{2\pi n x_i}{L}\right) + b_n \sin\left(\frac{2\pi n x_i}{L}\right)\right] \quad 1$$

Where: $Y_i(x)$ = Reading at x_i position
L = cross-sectional length of the anomaly
n = partial wave harmonic number
N = data points number
a_n = amplitude spectrum real part
b_n = amplitude spectrum imaginary part
i = 0, 1, 2, 3, ----------, n

} Partial Amplitude

and,

$$a_n = \frac{2}{N}\sum_{i=1}^{N} Y_i \cos\frac{2\pi n x_i}{L} \quad 2$$

$$b_n = \frac{2}{N}\sum_{i=1}^{N} Y_i \sin\frac{2\pi n x_i}{L} \quad 3$$

The work of Ikumbur et al. (2019) shows the main amplitude signal (A_n) as:

$$A_n = \sqrt{(a_n{}^2 + b_n{}^2)} \quad 4$$

A graph of A_n again frequency (n) was then plotted in the natural log graph and a linear trend of the low-frequency signal of the spectrum was plotted from the result and it shows the attributes of the deep-lying anomalous body. The gradient of the straight segment were analyzed and the depth to the subsurface anomalous body was calculated using the model developed by Tanaka *et al.* (1999):

$$z = -ML/2\pi \quad 5$$

where, z – basal depth ; M – slope of the linear section
L = anomalous body width

According to Usman *et al.* (2019); Okonkwo *et al.* (2012) Fourier transform methods are particularly useful in spatial data analysis such as the magnetic data. This present research focuses in appraising the geothermal energy potential of the RRWS region from the depth calculation and modelling of the basal depth of the magnetic bodies (Curie point depth) and heat flow around the region. The gradient of the computed wavelength signal of the outward average of the individual power spectrum was divided by the radial frequency to give depth to the center (centroid) of the anomalous deepest basal block (Zo). The depth to top (Zt) of the anomalous body was evaluated from the gradient of her second-longest wavelength part of the spectrum (Abraham *et al.* 2023 and Gobashy *et al.* 2023). A geothermal gradient model map and a 3D subsurface heat flow map were also generated from the calculated depth parameter values stated above.

$$\ln\left[\frac{\rho(\sqrt{S})}{/S/}\right] = \ln A - 2\pi/S/Z_o \quad (6)$$

ρ(s) is the radial average of the power
Z_0 is depth to the centroid
A = constant. (Abraham *et al,* 2014)

Biswas, 2015; Odoh et al. 2021 model was used to calculate the depth to the top (DTT) of the anomalous body (Zt).

$$In\left[\frac{\rho(\sqrt{S})}{/S/}\right] = InB - 2\pi/S/Z_t \quad (7)$$

B = sum of K without the gradient (Biswas and Acharya 2016)

Equation 8, Li. (2006) was deployed in calculating the depth to the bottom of the anomalous bodies.

$$Z_b = 2Z_o - Z_t \quad (8)$$

From the works of Abraham *et al.* (2019) and Li. (2006) the depth to bottom estimated is also the Curie point depth.

The heat flux density and thermal flow density for the region were estimated using Abraham *et al.* (2019); Li. (2006) and Usman *et al.* (2023) model (eq. 9).

$$q = \lambda\frac{dT}{dZ} \quad (9)$$

q = heat flux density and λ is the transferred heat coefficient. (Usman *et al.* 2023)
The work of Usman *et al.* (2023) was used to calculate the temperature gradient (equation 6).

$$\theta = \left[\frac{dT}{dZ}\right] Z_b \quad (10)$$

RESULTS

A qualitative interpretation was carried out by visually examining the total magnetic intensity (TMI) and residual anomalous map (RAM) (Fig. 3). High magnetic intensity was noted in the central and southeastern parts of the study area, particularly around Kare, Murai Bijimi, and Kauru. In contrast, lower magnetic intensity values were observed in the western, northern, and central regions, including the Rafin Rewa area (Fig. 3). The RAM map shows a general contour pattern trending from northeast to southwest (Fig. 3). Both the southern and northern sections of the study area exhibit high magnetic intensity. Research by Ikumbur *et al.* (2023) suggests that magnetic contrasts in faulted or fractured zones could be attributed to processes such as the oxidation of magnetite to hematite or the filling of fractures with vein deposits.

The visual analysis of the RAM map reveals that the central Rafin Rewa region has low magnetic intensity values, ranging from -5.57 to -82.3 nT, indicating the presence of thick sedimentary deposits in this area. In

contrast, regions like Kare, Murai Bijimi, and Kauru show high magnetic intensity values, ranging from 53.26 to 132.45 nT, suggesting thinner sedimentary layers. Additionally, the Ishemi area, located northwest of Rafin Rewa, also displays high magnetic intensity values, indicating a shallower sedimentary layer. The structural features of these interconnected regions suggest the potential for geothermal energy migration, as depicted in Figure 3.

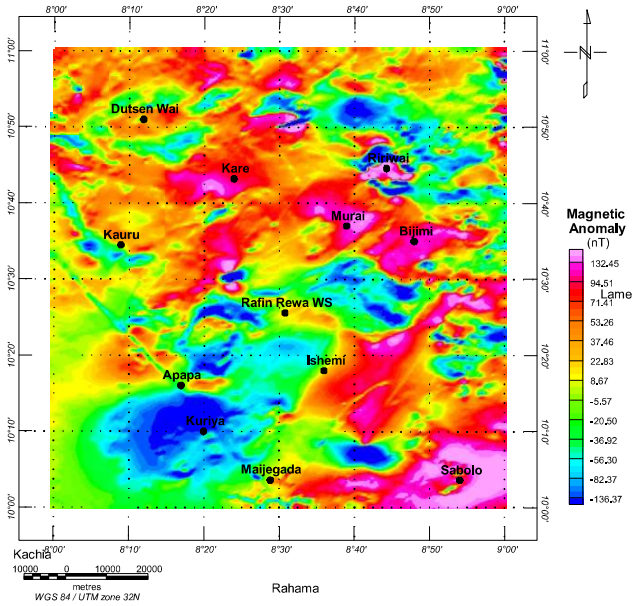

Figure 3: Residual magnetic anomalies at the Rafin Rewa Warm Spring region (RRWS).

Quantitative Interpretation

In this study, geophysical techniques such as spectral analysis and Euler deconvolution were utilized to estimate the depths and model the subsurface geological structures. The study area was divided into overlapping spectral blocks, each covering 37 km². Spectral analysis was performed on each block to derive the energy spectrum (Fig. 4). The focus of the investigation was to calculate the Depth to the Top (DTT) and Curie Point Depth (CPD) for the Rafin Rewa warm spring region, as shown in Table 1, Fig. 5, and Fig. 6. The DTT in this region ranges from 0.512 to 0.761 km, while the CPD varies between 6.504 and 10.582 km, with an average of 8.543 ± 0.325 km. Interestingly, both the CPD and DTT decrease as one moves further away from the Rafin Rewa warm spring. The average centroid depth is calculated to be 4.574 ± 0.042 km. The 3D model of the area shows that the sedimentary layer thins as it extends away from the warm spring, and its structure is undulating rather than flat (Fig. 9). Additionally, the 3D CPD model indicates that the sedimentary infill and the basal depth of the magnetic layer are controlled by structural factors, as depicted in Figs. 7 and 8.

For mapping subsurface structures, the Euler deconvolution technique was applied using structural indices (SI) of 0 and 1. This approach successfully identified and mapped the sill and dyke structures within the study area. With an SI of 0 (Fig. 10), two distinct depth sources were identified: deeper sources, representing areas with thick sedimentary deposits, and shallower sources, indicating regions with thin sedimentary infill. Magnetic source depths range from 220 to 1,196.48 meters, with the majority found outside the Rafin Rewa Warm Spring (RRWS) region. The subsurface geological structures predominantly follow an east-west (E-W) trend, and a high concentration of dyke-related solutions is located in the southern part of the study area (Fig. 10). Additionally, the Euler deconvolution analysis with an SI of 1 (Fig. 11) revealed fewer solutions within the RRWS region, while areas around Apapa and Ishemi exhibited higher concentrations, indicating significant structural activity and faulting in those regions.

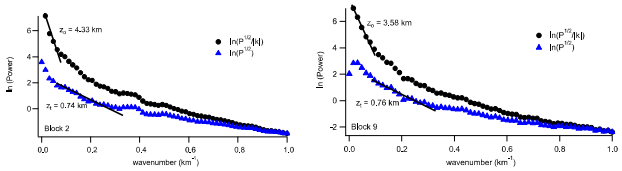

Figure 4: Sample spectral plots for radially average power spectrum computations (Blocks 2 and 9). Data from these spectra, derived from the windows analyzed, were used for the estimation of the CPD and subsequent heat flow computations.

Table 1: Results of spectral analysis computations and depth estimations of magnetic sources. Their accompanying error estimations are also presented.

Longitude	Latitude	Location Name	z_t (km)	Error z_t (±km)	z_o(km)	Error z_o (±km)	CPD (km)	Error CPD (±km)
8.25	10.75	Bugau	0.738	0.022	3.884	0.045	7.031	0.372
8.50	10.75	Zomo	0.741	0.023	4.329	0.023	7.916	0.331
8.75	10.75	Limi Hiris	0.512	0.016	4.836	0.029	9.160	0.387
8.75	10.50	Gunda	0.599	0.012	3.847	0.070	7.095	0.400
8.50	10.50	Rafin Gora	0.641	0.007	3.573	0.055	6.504	0.267
8.25	10.50	Babinda	0.593	0.011	4.113	0.023	7.633	0.230
8.25	10.25	Galadimawa	0.568	0.015	5.575	0.029	10.582	0.388
8.50	10.25	Shani	0.653	0.022	3.856	0.033	7.058	0.354
8.75	10.25	Ungwwar Gulawa	0.761	0.014	3.586	0.032	6.412	0.230

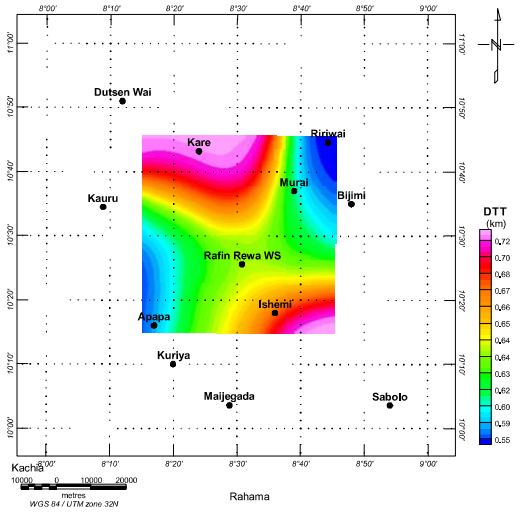

Figure 5: DTT of magnetic sources within the RRWS region. The depths increase away from the RRWS to the northern and southeastern regions of the RRWS region.

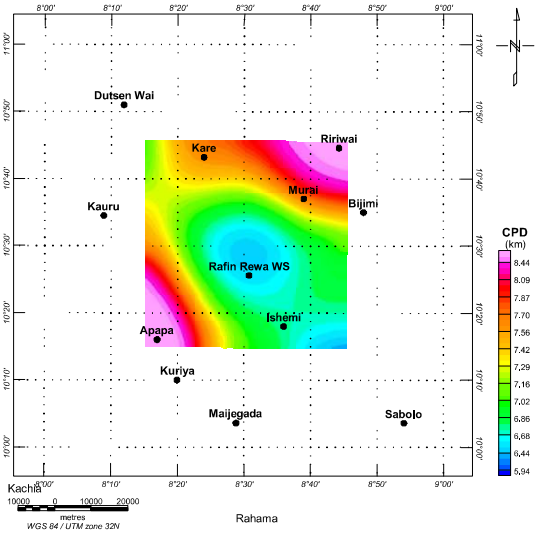

Figure 6: CPD results derived from the spectral analysis of aeromagnetic data from the region. The RRWS region indicates shallow CPD values between 6.44 and 6.6 km. The CPDs appear to increase away from the RRWS region.

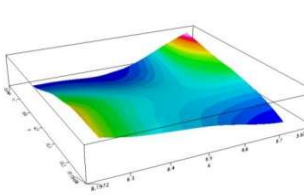

Figure 7: 3D representation of the DTT of magnetic sources.

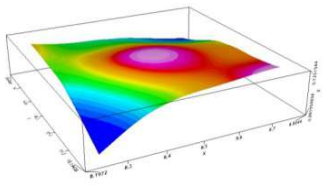

Figure 8: 3D representation of the estimated CPD in RRWS region.

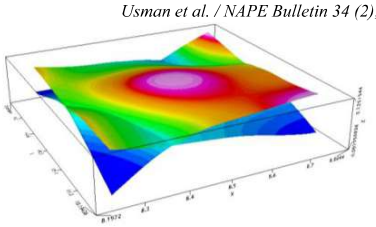

Figure 9: A combined representation of the DTT and CPD estimations from analysis of magnetic data from the RRWS region.

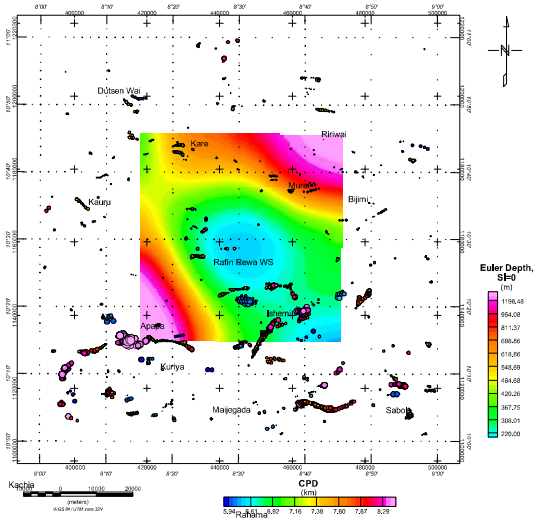

Figure 10: Euler depth results on the CPD map. The structural index SI = 0 investigates the existence of notable geological contacts (faults or fractures) in the region.

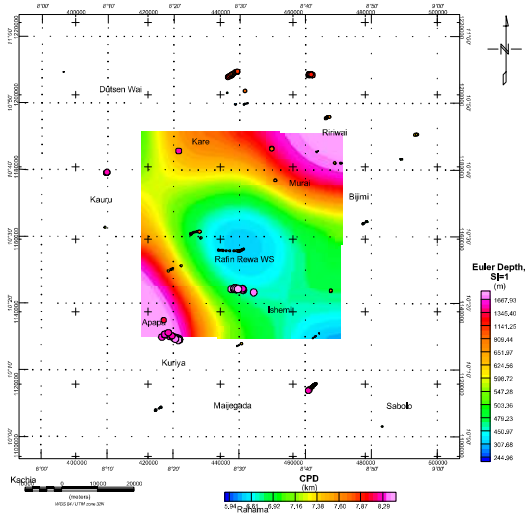

Figure 11: Euler depth results on the CPD map. The structural index SI = 1 investigates the existence of notable geological intrusions in the region.

Table 2: Results of laboratory analysis of the Rafin Rewa Warm Spring (Garba *et al*. 2012

Parameter	Samples from Rafin RewaAnalysed by GlownyInstytut Gornictwa,Katowice
PH	8.10
Electro– conductivity	350 µS/cm
Total Dissolved Solids	214 mg/l
Calcium	1.50 mg/l
Magnesium	0.06 mg/l
Sodium	88.51mg/l
Potassium	1.64 mg/l

Discussion

The magnetic anomalies in the study area (Fig. 3) reveal positive anomalies (> 53 nT) concentrated primarily in the central and southeastern regions, likely associated with the granitic rocks (Fig. 2). In contrast, low anomalies (< -1.5 nT) are identified around the Rafin Rewa Warm Spring (RRWS), likely linked to coastal plain sands from the Pliocene, Pleistocene, Oligocene, and Miocene eras. The low magnetic anomalies in the RRWS area may be partially influenced by the presence of a heat source. A similar observation was made by Abraham et al. (2014), who reported low magnetic anomalies at a warm spring site with comparable geological features to RRWS.

Data from Fig. 5 and Table 1 indicate that depths to the top (DTT) of magnetic sources range between 0.51 and 0.76 km. Shallow DTT values at RRWS average 0.63 km and increase toward the northern and southeastern parts of the study area. Notably, shallower DTT values (<0.55 km) were observed around Ririwai and Apapa, corresponding to granite formations in these areas. The study also found average Curie Point Depths (CPDs) between 6.41 ± 0.23 and 10.58 ± 0.39 km. At RRWS, CPDs range between 6.4 and 6.6 km and deepen towards the northeast and southwest. The shallow CPD at RRWS may be due to subsurface geologic intrusions within the undifferentiated basement complex, potentially contributing to the region's heat source. Similarly shallow CPDs are found south of RRWS in the Ishemi area, which sits on the undifferentiated basement complex and older Pan-African granites. These regions, with shallow CPDs, are promising targets for further geothermal exploration.

The 3D model of the estimated depths (Figs. 7, 8, and 9) indicates a clear subsurface intrusion, with shallower depths at RRWS compared to other areas. A notable depression in the DTT, nearly intersecting with the CPD plot at RRWS (Fig. 9), suggests high heat flow in this region. This theory is supported by an average heat flow of 160.76 ± 19.09 mW/m², as heat flow values exceeding 80 to 100 mW/m² typically signal anomalous geothermal conditions, warranting further investigation (Abraham et al., 2014, 2018, 2019). The existence of RRWS supports this deduction. Additionally, an analysis of geological contacts' influence on CPD results (Fig. 10) shows minimal surface impact. Clusters of solutions from Euler deconvolution suggest geological contacts that may represent faults or fractures within RRWS at depths of 480 to 618 meters, trending east-west (E-W) and northeast-southwest (NE-SW). Fig. 11 indicates possible subsurface intrusions at depths of 547 to 1,700 meters, potentially representing granitic rock intrusions in the RRWS region.

Geochemical analysis of the RRWS (Table 2) shows a pH of 8.1, indicating slightly alkaline subsurface fluids. This alkalinity may facilitate mineral dissolution in subsurface rocks, influencing porosity, permeability, thermal conductivity, and heat transfer properties. The electro-conductivity value of 350 S/cm (Table 2) suggests the presence of ions and moderate salinity, which can impact the water's thermal behavior and heat transfer efficiency. Total Dissolved Solids (TDS) of 214 mg/l reflect the concentration of dissolved substances, which can influence thermal conductivity and heat capacity. The presence of ions such as calcium (2.6 mg/l), magnesium (4.4 mg/l), sodium (0.71 mg/l), and potassium (0.84 mg/l) (Table 2) is linked to the thermal behavior of the fluids, affecting heat transfer processes. These variations in ionic composition play a role in fluid circulation, heat exchange, and the overall thermal regime of the RRWS area.

CONCLUSION

The Rafin Rewa Warm Spring (RRWS) region was investigated using integrated geophysical techniques, including Spectral Analysis and Euler deconvolution. Qualitative magnetic data suggests shallow basal depths near RRWS, with increasing magnetism moving outward, while the sedimentary layers display uneven, undulating features shaped by local structures. Quantitative analysis links heat flow density to subsurface formations, identifying potential conduits for heat transfer. A 3D model, combining Depth to the Top (DTT) and Curie Point Depth (CPD), reveals a heat flow depression near RRWS, with CPDs averaging between 6.41 ± 0.23 km and 10.58 ± 0.39 km. These shallow CPDs suggest possible subsurface intrusive activity and elevated heat flow, highlighting the geothermal exploration potential. The region's average heat flow of 160.76 ± 19.09 mW/m² exceeds typical geothermal thresholds, which are usually between 80 and 100 mW/m², supporting the need for further study. These findings align with previous research by Abraham et al. (2014, 2018, 2019) and warrant deeper investigation. Euler deconvolution results show faults and fractures at depths of 480–618 meters, trending east-west (E-W) and northeast-southwest (NE-SW). Fluid composition

analysis indicates an impact on convective heat transfer, reinforcing the geothermal potential of the RRWS area.

REFERENCES CITED

Abraham, E., Usman, A., Chıma, K., Azuoko, G. & Ikeazota, I. (2023). Magnetic inversion modeling of subsurface geologic structures for mineral deposits mapping in southeastern Nigeria. Bulletin of the Mineral Research and Exploration, 1-1. DOI: 10.19111/bulletinofmre.1267876

Abraham, E. M. and Owens M. Alile (2019). Modelling Subsurface Geologic Structures at Ikogosi Geothermal Field, Southwestern Nigeria, using Gravity, Magnetics, and Seismic Interferometry Techniques (2019). Journal of Geophysics and Engineering 16, 729–741.https://academic.oup.com/jge/advance-article-abstract/doi/10.1093/jge/gxz034/5531815.

Abraham, E., Itumoh, O., Chukwu, C., Rock, O. (2018). Geothermal Energy Reconnaissance of Southeastern Nigeria from Analysis of Aeromagnetic and Gravity Data. Pure and Applied Geophysics, 176: 22 – 36. https://doi.org/10.1007/s00024-018-2028-1

Abraham, E., Itumoh, O., Chukwu, C., Rock, O. (2018). Geothermal Energy Reconnaissance of Southeastern Nigeria from Analysis of Aeromagnetic and Gravity Data. Pure and Applied Geophysics, 176: 22 – 36.https://doi.org/10.1007/s00024-018-2028-1

Abraham, E. M., Nkitnam, E. E. (2017). Review of geothermal energy research in Nigeria: The geoscience front. Int. J. Earth Sci. Geophys 3: 015

Abraham, E. M., Obande, E. G., Mbazor, C., Chibuzo, G. C. and Mkpuma, R. O. (2015). Estimating depth to the bottom of magnetic sources at Wikki Warm Spring region, northeast Nigeria using fractal distribution of sources approach. Turkish Journal of Earth Sci. 24: 1 - 19. DOI: 10.3906/yer-1407-12

Abraham, E. M., Lawal, K. M., Ekwe, A. C., Alile, O., Murana, K. A., Lawal, A. A., (2014). Spectral analysis of aeromagnetic data for geothermal energy investigation of Ikogosi warm spring – Ekiti State, southwestern Nigeria. Geothermal Energy 2:6. 1-21. https://doi.org/10.1186/s40517-014-0006-0

Biswas A (2015) Interpretation of residual gravity anomaly caused by a simple shaped body using very fast simulated annealing global optimization. Geoscience Frontiers, 6(6), p 875-893.

Chinwuko A. I, Usman A. O, Onwuemesi A. G, Anakwuba E. K, Okonkwo C. C and Ikumbur E. B (2014) Interpretations of aeromagnetic data over lokoja and environs, Nigeria. International Journal of Advanced Geosciences. 2 (2), 66- 71

Chukwu, C.G., Udensi, E.E., Abraham, E.M., Ekwe, A.C and A.O. Selemo, Geothermal Energy Potential from Analysis of Aeromagnetic Data of Part of The Niger-Delta Basin, Southern Nigeria, Energy (2017), doi:10.1016/j.energy.2017.11.040

Gobashy M. M, Eldougdoug A, Abdelwahed M (2023) Role of Integrated Magnetics and Geology in Tracking and Exploring Complex Structures Controlling Gold Mineralization. Example from the Fawakheir-Atalla Gold Prospects, Eastern Desert, Egypt. Pure Appl. Geophys. 180: 2775–2805

Garba, M. L., Kurowska, E., Schoeneich, K and Abdullahi, I (2012). Rafin Rewa Warm Spring, A New Geothermal Discovery. American International Journal of Contemporary Research 2, 9: 231-235

Ikumbur E. B, Onwuemesi A. G, Anakwuba E. K, Chinwuko A. I and Usman A. O (2023) Evaluation of Geothermal Energy Potential of Parts of the Middle Benue Trough Nigeria: Aeromagnetic and Aeroradiometric Approach. Iranian Journal of Geophysics, 16 (4): 7-52

Kamal Abdelrahman, Stephen E. Ekwok, Christian A. Ulem, Ahmed M. Eldosouky, Naif Al-Otaibi, Bashar Y. Hazaea, Saddam Ali Hazaea, Peter Andráš and Anthony E. Akpan (2023). Exploratory Mapping of the Geothermal Anomalies in the Neoproterozoic Arabian Shield, Saudi Arabia, Using Magnetic Data. Minerals 13(5), 694; https://doi.org/10.3390/min13050694

Li X (2006) Understanding 3D analytic signal amplitude. Geophysics 71(2): L13–L16, 1 FIG. https:// doi. org/ 10. 1190/1. 21843 67

Nwajide, C.S., 2005. Geology of Nigeria's Sedimentary Basins. CSS Bookshop Ltd., Lagos, 1-565.

Obaje, N. G., 2009, Geology and Mineral Resources of Nigeria, Lecture Notes in Earth Sciences, Springer, Berlin Heidelberg.

Odoh O P, Ezeh C. C, Usman A. O., Okanya O. S and Chima C. J (2021) Delineation of Basin Geometry within Parts of Northern Anambra Basin, Nigeria: An Aeromagnetic Approach Journal of Environment and Earth Science. 11, 4, 28-39

Okonkwo C. C, Onwuemesi A. G, Anakwuba E. K, Chinwuko A. I, Ikumbur B. E, Usman A. O (2012) Aeromagnetic Interpretation over Maiduguri and Environs of Southern Chad Basin, Nigeria. Journal of Earth Sciences and Geotechnical Engineering, vol.2, no. 3, 77-93

Stephen E. Ekwok, Ahmed M. Eldosouky, Ogiji-Idaga M. Achadu, Anthony E. Akpan, Luan Thanh Pham, Kamal Abdelrahman, David Gómez-Ortiz, Ubong C. Ben, Mohammed S. Fnais (2022). Application of the enhanced horizontal gradient amplitude (EHGA) filter in mapping of geological structures involving magnetic data in southeast Nigeria, Journal of King Saud University - Science, Volume 34, Issue 8, 102288, https://doi.org/10.1016/j.jksus.2022.102288.

Tanaka, A.Y., Okubo, Y. and Matsubayashi, O., 1999. Curie point depth based on spectrum analysis of the magnetic anomaly data in East and Southeast Asia, Tectonophysics, vol. 396, pp. 461-470.

Usman A. O, Ezeh C. C and Chinwuko A. I (2019) Estimation of Geothermal gradient and Curie Point Depth for Delineating Hydrocarbon potentials zones over Southern Bida Basin, Northwestern Nigeria. Development Journal of Science and Technology Research (DJOSTRR). 8,1. 105-119

Usman A. O, Chinwuko A. I, Azuoko G. B, Ekwe A. C, Abraham E. M and Chizoba C. J (2023) Geo-morphological mapping of the Basin configuration of parts of Southern Nupe Basin, Nigeria using High-Resolution Aeromagnetic and core drill dataset. Iranian Journal of Geophysics, Accepted April 8th 2023

Wikipedia (2016). List of Power stations in Nigeria. https://en.wikipedia.org/wiki/List-of-power-stations-in-Nigeria#cite-ref-1